

Characterization of topological phase transitions via topological properties of transition points

Linhu Li¹ and Shu Chen^{1,2,*}

¹*Beijing National Laboratory for Condensed Matter Physics,
Institute of Physics, Chinese Academy of Sciences, Beijing 100190, China*
²*Collaborative Innovation Center of Quantum Matter, Beijing, China*

We study topological properties of phase transition points of topological quantum phase transitions by assigning a topological invariant defined on a closed circle or surface surrounding the phase transition point in the parameter space of momentum and transition driving parameter. By applying our scheme to the Su-Schrieffer-Heeger model and Haldane model, we demonstrate that the topological phase transition can be well characterized by the defined topological invariant of the transition point, which reflects the change of topological invariants of topologically different phases across the phase transition point.

PACS numbers: 03.65.Vf, 64.60.-i, 05.70.Fh

I. INTRODUCTION

Conventional continuous quantum phase transitions (QPTs) are driven by pure quantum fluctuation effects due to the change of external parameters and generally described in terms of the spontaneous symmetry breaking and order parameters of the ground state¹. On the contrary, topological QPTs involve the change of ground-state topological properties and accompany no symmetry breaking²⁻⁴. Different topological states are classified by topological quantum numbers, which take discrete numbers, in contrast to order parameters used in conventional QPTs to distinguish various phases, which generally take continuous values. Conventionally, continuous QPTs can be classified into different order QPTs by singularity properties of the ground-state energy at the phase transition point (or critical point for $n \geq 2$), i.e., n th order QPTs are characterized by discontinuities in the n th derivative of the ground-state energy.

As the singularity of ground-state energy plays an important role in determining universal properties around the critical point of the QPT, however it can not distinguish whether the phase transition is a topological QPT or a conventional one within the Landau-Ginzburg paradigm¹. Beyond the traditional energy criterion, a QPT can be also witnessed by qualitative changes of physical quantities related to the ground-state wavefunctions, e.g., the Berry phase^{5,6}, quantum fidelity and the fidelity susceptibility⁷⁻¹⁰, and the quantum geometric tensor¹¹⁻¹³. Although these approaches have shed light on our understanding of QPTs from the geometric aspect of the ground-state manifold, one can not identify a QPT to be a topological or trivial one solely from the singularity of particular physical quantities at the phase transition point unless additional quantities related to the topological invariant are calculated. An interesting question arising here is whether we can characterize a QPT is topological or conventional phase transition from the property of the phase transition point?

To answer the question, let us recall that a topological QPT distinguished from a trivial one is manifested by the change of topological invariant, instead of symmetry breaking, across the transition point. While the topological invariant, e.g., the quantized Berry phase for one-dimensional (1D) topological systems¹⁴ or Chern number for two-dimensional (2D) quan-

tum Hall systems¹⁵, is well defined for a gapped phase apart from the QPT point and characterizes the global geometrical property of the Bloch band, it fails to work at the gapless critical point. To overcome the difficulty, in this work we propose an alternative definition for the topological invariant, which is not defined on the momentum space at the transition point, but via a closed detour path surrounding the critical point on the parameter space spanning by both the momentum and the transition driving parameter. By applying this idea to the 1D and 2D topological systems, e.g., the celebrated Su-Schrieffer-Heeger (SSH) model and Haldane model, we demonstrate these topological invariants taking nontrivial quantized numbers for topological QPTs, but some non-universal numbers or zero number for conventional QPTs. Our results suggest that we can judge topological or trivial QPTs from topological properties of the phase transition points.

II. MODELS AND RESULTS

A. 1D topological models

We begin our discussion with one of the simplest 1D topological systems, the SSH model¹⁶, which can be described by the Hamiltonian:

$$H = \sum_i [(t + \delta)\hat{c}_{A,i}^\dagger \hat{c}_{B,i} + (t - \delta)\hat{c}_{A,i+1}^\dagger \hat{c}_{B,i}] + h.c., \quad (1)$$

where $\hat{c}_{A(B),i}^\dagger$ is the creation operator of fermion on i -th A (or B) sublattice. This model has two sites in a unit cell, the hopping amplitude in the unit cell is $t + \delta$ and that between two unit cells is $t - \delta$. For convenience, $t = 1$ is taken as the energy unit. After the Fourier transformation $\hat{c}_{s,j} = \frac{1}{\sqrt{L}} \sum_k e^{ikj} \hat{c}_{k,s}$ with $s = A(B)$, the Hamiltonian can be written as

$$H = \psi_k^\dagger h(k) \psi_k, \quad (2)$$

where $\psi_k^\dagger = (\hat{c}_{k,A}^\dagger, \hat{c}_{k,B}^\dagger)$ and $h(k) = h_x \sigma_x + h_y \sigma_y$ with σ the Pauli matrix acting on the vector ψ_k , $h_x = (1 + \delta) + (1 - \delta) \cos k$, $h_y = (1 - \delta) \sin k$. It is well known that this model belongs to the BDI class according to the standard topological classification¹⁷ and has two topologically distinct phases for

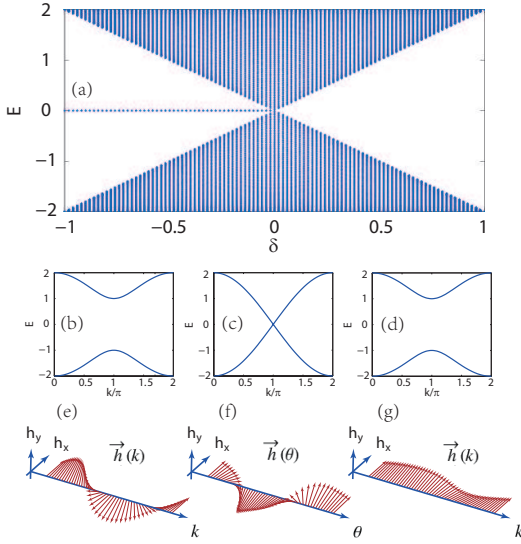


FIG. 1: (Color online) (a) The spectrum of the SSH model versus δ under OBC. (b)-(d) The spectrum versus k under PBC, with (b) $\delta = -0.5$, (c) $\delta = 0$ and (d) $\delta = 0.5$. (e) and (g) show the winding of $h(k)$ across the Brillouin zone, corresponding to (b) and (d) respectively. (f) shows the winding of $h(\theta)$ as θ varies a period. The arrows in (e)-(g) show the direction of the Hamiltonian $h(k)$ and $h(\theta)$.

$\delta > 0$ and $\delta < 0$ with the phase transition point at $\delta = 0$, where the gap closes at $k = \pi$. Under the open boundary condition (OBC), these two phases can be distinguished by the presence and absence of degenerate zero-mode edge states¹⁸, as shown in Fig.1(a).

While the spectrum under periodic boundary condition (PBC) shows a similar structure for $\delta < 0$ or $\delta > 0$, as displayed in Fig.1(b)-(d), the topological property of the distinct phase can be characterized by the Zak phase^{21,22}, i.e., the Berry phase across the Brillouin zone, which is defined as

$$\gamma = i \int_{-\pi}^{\pi} dk \langle \varphi(k) | \partial_k | \varphi(k) \rangle, \quad (3)$$

with $\varphi(k)$ the eigenstate of the occupied Bloch band. While the topological phase is characterized by $\gamma = \pi$ for $\delta < 0$, the trivial phase corresponds to $\gamma = 0$ for $\delta > 0$. The geometrical meaning of the Zak phase can be understood as the winding angle of $h(k)$ as k varies across the Brillouin zone²³, as shown in Fig.1(e) and (g). For the topological nontrivial case with $\delta = -0.5$, the direction of $h(k)$ winds an angle of 2π , whereas for the trivial case with $\delta = 0.5$ the winding angle is zero. However, when $\delta = 0$, the two bands are degenerate at $k = \pi$ (Fig.1(c)), and the Zak phase is ill-defined.

To describe the topological property of state at the phase transition point, here we defined the Berry phase on a circle around the gap closing point in the parameter space of k and δ . Introducing θ as the varying angle and A as radius of the circle, we have $k = A \sin \theta + \pi$ and $\delta = A \cos \theta$, hence the Hamiltonian around the circle can be represented as $h(\theta)$, and

the Berry phase is defined as

$$\gamma_d = i \int_{-\pi}^{\pi} d\theta \langle \varphi(\theta) | \partial_\theta | \varphi(\theta) \rangle. \quad (4)$$

After some algebras, one can obtain $\gamma_d = \pi$, which corresponds to the topological phase transition at $\delta = 0$. In Fig.1(f), we also show the winding of $h(\theta)$ as θ varies a period, giving rise to a winding angle of 2π .

As a comparison, we next consider a topologically trivial two-band model with alternating on-site potentials, described by the Hamiltonian:

$$H = \sum_i t[\hat{c}_{A,i}^\dagger \hat{c}_{B,i} + \hat{c}_{A,i+1}^\dagger \hat{c}_{B,i} + h.c.] + \mu(\hat{c}_{A,i}^\dagger \hat{c}_{A,i} - \hat{c}_{B,i}^\dagger \hat{c}_{B,i}). \quad (5)$$

This model has alternating chemical potential μ and $-\mu$ for site A and B, and has a similar spectrum as the SSH model with a phase transition occurring at $\mu = 0$. However, as μ breaks the inversion symmetry, the Berry phase of each band is no longer quantized and no degenerate edge states emerge under the OBC. Similarly, we can also calculate the Berry phase around the gap closing point at $\mu = 0$ and $k = \pi$. The numerical result shows that γ_d is not a quantized invariant and is associated with the radius A of the integral path. On the contrary, the γ_d for the SSH model is always π regardless of the value of A , which suggests that γ_d is a topological invariant. This difference means that we can judge whether the QPT is a topological phase transition from values of the Berry phase γ_d around the critical point.

Similar scheme can be directly applied to the other 1D topological nontrivial systems with the ground state characterized by the Z-type invariant. According to the ten-fold-way classification¹⁷, in one dimension the BDI (orthogonal), AIII (unitary) and CII (symplectic) classes belong to the Z type. As the SSH model belongs to the BDI class, next we consider the fermionic Creutz ladder^{19,20}, which is related to the 1D AIII topological insulator. The Creutz ladder can be described by the Hamiltonian:

$$H = \sum_i K e^{-i\alpha} \hat{c}_{A,i+1}^\dagger \hat{c}_{A,i} + K e^{i\alpha} \hat{c}_{B,i+1}^\dagger \hat{c}_{B,i} + K \hat{c}_{B,i+1}^\dagger \hat{c}_{A,i} + K \hat{c}_{A,i+1}^\dagger \hat{c}_{B,i} + M \hat{c}_{A,i}^\dagger \hat{c}_{B,i} + h.c., \quad (6)$$

where K and M are tunneling strengths, α is a magnetic flux, and $K = 1$ is set to be the energy unit. In the momentum space, the Hamiltonian $h(k)$ is given by $h(k) = h_0 I + h_x \sigma_x + h_z \sigma_z$, with $h_0 = 2 \cos \alpha \cos k$, $h_x = 2 \cos k + M$, $h_z(k) = -2 \sin \alpha \sin k$. Generally, this model has no time-reversal symmetry due to the introduction of α . For the specific case with $\alpha = \pm\pi/2$, one can check that the Hamiltonian fulfills the chiral symmetry $\sigma_y h(k) \sigma_y = -h(k)$, which means the system with $\alpha = \pm\pi/2$ belonging to the AIII class. This model also has a two-band spectrum, and the gap closes when $\sin \alpha = 0$, $M = -2 \cos k$ or $M = \pm 2$, $\cos k = \mp 1$. The phase diagram is shown in Fig.2, which indicates the phase within the parameter regime of $|M| < 2$ is topologically nontrivial characterized by the Zak phase $\gamma = \pm\pi$, whereas the phase with $|M| > 2$ is a trivial phase with $\gamma = 0$. Notice that although the Zak phase usually

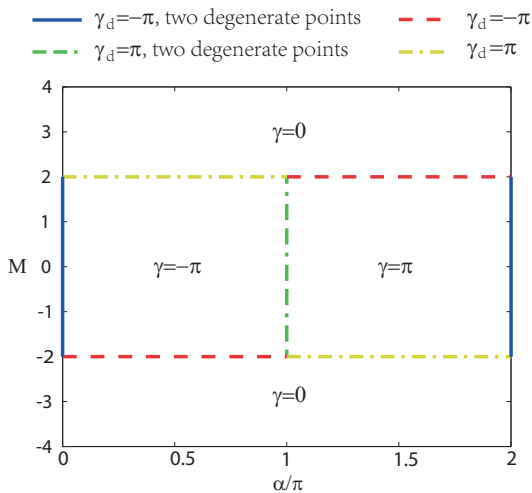


FIG. 2: (Color online) The phase diagram of the Creutz ladder model with γ_d on the phase boundary being marked. There are two degenerate points in the Brillouin zone for the system with $|M| < 2$ and $\alpha = \pi$ or 0 , and the summation of γ_d is $\pm 2\pi$.

only takes 0 or π with a modulus 2π , the winding directions of $h(k)$ are opposite to each other for $\gamma = \pi$ and $\gamma = -\pi$, which represent different topological phases. It is interesting to point out that the state at $\alpha = 0$ and π within $|M| < 2$ is a 1D semimetal with band touching points at $k = \pm \arccos(-M/2)$. At the phase boundary $M = \pm 2$, which separates the trivial and topological phases, the band gap closes at $k = \pi$ or 0 . Similar to Eq.(4), we can calculate the Berry phase around the gap closing point at $(M = 2, k = \pi)$ or $(M = -2, k = 0)$. As displayed in Fig.2, we have $\gamma_d = \pm\pi$ at the phase boundary, which corresponds to the change of the Zak phase γ at different phases. If we fix M and take α as a driving parameter, we can calculate the Berry phase around the band touching points ($\alpha = 0, k = \pm \arccos(-M/2)$) or ($\alpha = \pi, k = \pm \arccos(-M/2)$). For $\alpha = 0$, we get $\gamma_d = -\pi$ at both gap closing points, and for $\alpha = \pi$ we get $\gamma_d = \pi$. It is clear that the summation of γ_d for these two degenerate points gives -2π or 2π , consistent with the change of the Zak phase γ at different sides of $\alpha = 0$ or $\alpha = \pi$.

We have indicated that the Creutz ladder system with $\alpha = \pm\pi/2$ belongs to the AIII class. When α deviates $\pm\pi/2$, the chiral symmetry is broken and the system can not be classified into the standard ten-fold classes¹⁷. Nevertheless, the system still supports topologically nontrivial phase with the Zak phase $\gamma = \pm\pi$ as the system is protected by the inversion symmetry^{21,24}, i.e., $\sigma_x h(k) \sigma_x = h(-k)$. Through the above examples, it is clear that our scheme works for both the standard topological classes, e.g., the BDI class and the AIII class, and the non-standard class protected by other symmetries as long as the topological phase can be characterized by a nontrivial Berry phase.

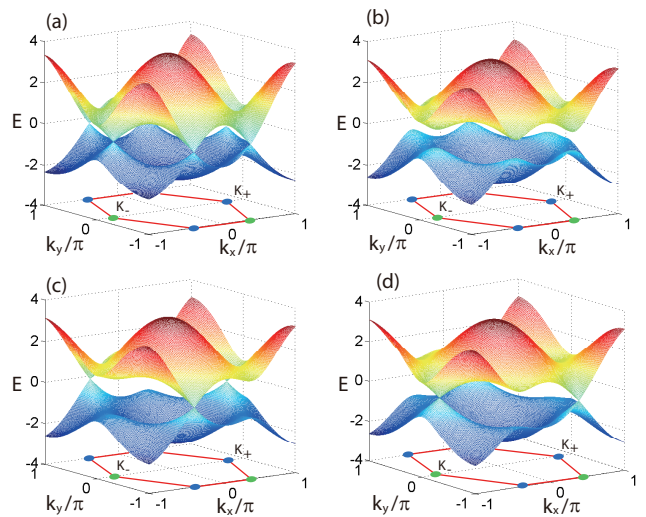


FIG. 3: (Color online) The energy spectrum of the Haldane model with $t_1 = 1$ and $t_2 = 0.1$. (a) $M = 0, \alpha = 0$; (b) $M = 0, \alpha = \pi/3$; (c) $M = 3\sqrt{3}t_2 \sin \alpha, \alpha = \pi/3$; (d) $M = -3\sqrt{3}t_2 \sin \alpha, \alpha = \pi/3$. (a), (c) and (d) are on the phase boundary, while (b) is in the gap opened region. The gap closes at both Dirac points in (a), while it closes only at one of the two Dirac points in (c) and (d), respectively.

B. 2D topological models

Next we apply a similar scheme to study the topological property of phase transition points of 2D systems. We begin our discussion with the famous Haldane model²⁵, which supports a rich phase diagram, exhibiting either topological or trivial phase transitions. The Haldane model is a prototype model which may realize the anomalous quantum Hall effect in a 2D honeycomb lattice without any net magnetic flux through a unit cell of the system. The Hamiltonian of the Haldane model is given by:

$$H = \sum_i t_0 \hat{c}_i^\dagger \hat{c}_i + \sum_{\langle i,j \rangle} t_1 \hat{c}_i^\dagger \hat{c}_j + \sum_{\langle\langle i,j \rangle\rangle} t_2 e^{i\alpha_{i,j}} \hat{c}_i^\dagger \hat{c}_j, \quad (7)$$

where the summation is defined on the 2D honeycomb lattice, which is composed of two sublattices labeled by A and B, respectively. Here $t_0 = M$ for site A and $t_0 = -M$ for site B, t_1 denotes the nearest-neighbor hopping amplitude, and t_2 denotes the next-nearest-neighbor (NNN) hopping amplitude. The magnitude of the phase is set to be $|\alpha_{i,j}| = \alpha$, and the direction of the positive phase is clockwise, following Haldane's work. This model is well known for its three topologically different phases characterized by the Chern number C ($C = \pm 1$ or 0), which is defined as the integral of the Berry curvature \mathbf{V} for each band in the Brillouin zone, with \mathbf{V} defined as $\nabla \times i\langle \varphi(\mathbf{k}) | \nabla | \varphi(\mathbf{k}) \rangle$, where $\varphi(\mathbf{k}) = \varphi(k_x, k_y)$ is the eigenstate of the occupied Bloch band.

Consider the case with $|t_2/t_1| < 1/3$, for which the two bands never overlap and only touch at the Brillouin zone corner when $M = \mp 3\sqrt{3}t_2 \sin \alpha$. Expanding the Hamiltonian in the momentum space around the Dirac point $\mathbf{K}_\pm = (\pm \frac{4\pi}{3\sqrt{3}}, 0)$, i.e. $k_x = \pm \frac{4\pi}{3\sqrt{3}} + x$ and $k_y = y$, we get the effective

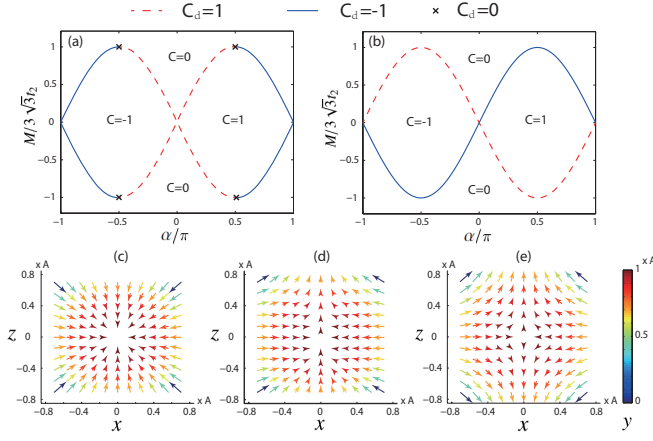


FIG. 4: (Color online) (a) and (b) show the phase diagram of the Haldane model with C_d on the phase boundary being marked. (a) is for the case with C_d defined in the space of momentum and α ; (b) is for the case with C_d defined in the space of momentum and M . (c)-(e) show the direction of $h(\mathbf{k})$ near the gap closing point in (a) with different α_0 : (c) $\alpha_0 = \pi/3$, $M = 9t_2/2$, $C_d = 1$; (d) $\alpha_0 = \pi/2$, $M = 3\sqrt{3}t_2$, $C_d = 0$; (e) $\alpha_0 = 2\pi/3$, $M = 9t_2/2$, $C_d = -1$.

Hamiltonian:

$$h(\mathbf{k}) = \mp \sqrt{3}t_1 x \sigma_x + t_1 y \sigma_y + (M \mp 3\sqrt{3}t_2 \sin \alpha) \sigma_z. \quad (8)$$

The gap closing points are at $x = y = 0$ and $M \mp 3\sqrt{3}t_2 \sin \alpha = 0$. While the gap closes at both of \mathbf{K}_{\pm} when $M = 0$ and $\alpha = 0$ or π , there can be no more than one gap closing point for other value of α , i.e., the gap closes at \mathbf{K}_+ when $M = 3\sqrt{3}t_2 \sin \alpha$ or at \mathbf{K}_- when $M = -3\sqrt{3}t_2 \sin \alpha$. Different situations of band touching are shown in Fig.3.

The phase diagram of Haldane model is displayed in Fig.4 (a) or (b) with different phases characterized by the Chern number C . At the phase boundary, the gap between the upper and lower energy bands closes, and the Chern number is ill-defined therein. Similar to the 1D case, we can define a topological invariant on a closed surface surrounding the phase transition point in the parameter space of \mathbf{k} and transition driving parameter δ to describe the topological property of the transition point. Different from the 1D system, here the topological invariant is given by

$$C_d = -\frac{1}{2\pi} \oint \mathbf{V} \cdot d\mathbf{S}, \quad (9)$$

with \mathbf{S} a sphere surface around the gap closing point (k_x^0, k_y^0, δ_0) . Following Berry's work²⁶, the Berry curvature for the lower band can be expressed as:

$$\mathbf{V} = \text{Im} \frac{\langle -|\nabla h(\mathbf{k}, \delta)|+\rangle \times \langle +|\nabla h(\mathbf{k}, \delta)|-\rangle}{(E_- - E_+)^2}, \quad (10)$$

with $|+\rangle$ ($|-\rangle$) the eigenstate of the upper (lower) band. With some further calculations, the Berry curvature can be written

as:

$$\begin{aligned} V^x &= -\frac{1}{2R^3} \left[\frac{\partial h_x}{\partial k_y} \frac{\partial h_y}{\partial \delta} h_z + \frac{\partial h_y}{\partial k_y} \frac{\partial h_z}{\partial \delta} h_x + \frac{\partial h_z}{\partial k_y} \frac{\partial h_x}{\partial \delta} h_y \right. \\ &\quad \left. - \frac{\partial h_y}{\partial k_y} \frac{\partial h_x}{\partial \delta} h_z - \frac{\partial h_x}{\partial k_y} \frac{\partial h_z}{\partial \delta} h_y - \frac{\partial h_z}{\partial k_y} \frac{\partial h_y}{\partial \delta} h_x \right], \\ V^y &= -\frac{1}{2R^3} \left[\frac{\partial h_x}{\partial \delta} \frac{\partial h_y}{\partial k_x} h_z + \frac{\partial h_y}{\partial \delta} \frac{\partial h_z}{\partial k_x} h_x + \frac{\partial h_z}{\partial \delta} \frac{\partial h_x}{\partial k_x} h_y \right. \\ &\quad \left. - \frac{\partial h_y}{\partial z} \frac{\partial h_x}{\partial k_x} h_z - \frac{\partial h_x}{\partial z} \frac{\partial h_z}{\partial k_x} h_y - \frac{\partial h_z}{\partial z} \frac{\partial h_y}{\partial k_x} h_x \right], \\ V^z &= -\frac{1}{2R^3} \left[\frac{\partial h_x}{\partial k_x} \frac{\partial h_y}{\partial k_y} h_z + \frac{\partial h_y}{\partial k_x} \frac{\partial h_z}{\partial k_y} h_x + \frac{\partial h_z}{\partial k_x} \frac{\partial h_x}{\partial k_y} h_y \right. \\ &\quad \left. - \frac{\partial h_y}{\partial k_x} \frac{\partial h_x}{\partial k_y} h_z - \frac{\partial h_x}{\partial k_x} \frac{\partial h_z}{\partial k_y} h_y - \frac{\partial h_z}{\partial k_x} \frac{\partial h_y}{\partial k_y} h_x \right]. \end{aligned}$$

Here the Hamiltonian $h(\mathbf{k}) = h_x \sigma_x + h_y \sigma_y + h_z \sigma_z$ and $R = \sqrt{h_x^2 + h_y^2 + h_z^2}$. For convenience, we choose a spherical surface surrounding the gap closing point with a radius of A , i.e., $k_x = k_x^0 + x$, $k_y = k_y^0 + y$, $\delta = \delta_0 + z$ with $x = A \sin \theta \cos \phi$, $y = A \sin \theta \sin \phi$ and $z = A \cos \theta$, where θ is the polar angle and ϕ is the azimuthal angle of the spherical surface. The integral then becomes:

$$C_d = -\frac{1}{2\pi} \oint \mathbf{V} \cdot (\sin \theta \cos \phi, \sin \theta \sin \phi, \cos \theta) A^2 \sin \theta d\theta d\phi.$$

If all the h_x , h_y and h_z are linear of (x, y, z) around a gap closing point, we can rotate and stretch the axes to reach $h_x = \pm x$, $h_y = \pm y$, $h_z = \pm z$, and the Chern number $C_d = \pm 1$.

As the phase boundary is given by $|M| = 3\sqrt{3}|t_2 \sin \alpha|$, either the parameter α or M can be chosen as the phase transition driving parameter. Similar to the 1D cases, we can judge whether the phase transition is topological or not by examining C_d defined around the gap closed points. First we choose α as the third parameter besides the momentum \mathbf{k} by keeping M fixed. We take the case with the transition point located at \mathbf{K}_+ as an example, and the case at \mathbf{K}_- can be analyzed similarly. Defining $\alpha = \alpha_0 + z$ with $M - 3\sqrt{3}t_2 \sin \alpha_0 = 0$ and expanding the Hamiltonian near α_0 , we have

$$h(\mathbf{k}) = -\sqrt{3}t_1 x \sigma_x + t_1 y \sigma_y - 3\sqrt{3}t_2 \cos \alpha_0 z \sigma_z \quad (11)$$

when $|M| < 3\sqrt{3}|t_2|$, and the Chern number around \mathbf{K}_+ is $C_d(\alpha) = \text{sgn}(\cos \alpha_0)$. When $|M| = 3\sqrt{3}|t_2|$, i.e., the case with $\alpha_0 = \pm\pi/2$ marked by the ‘‘cross’’ in Fig.4(a), however, the expansion becomes

$$h(\mathbf{k}) = -\sqrt{3}t_1 x \sigma_x + t_1 y \sigma_y + 3\sqrt{3}t_2 z^2 \sigma_z, \quad (12)$$

and the integral results in $C_d(\alpha) = 0$ as the integrand is an odd function in the interval. In Fig.4(a), we show the value of C_d around the phase boundary: except $C_d = 0$ at the four points marked by ‘‘crosses’’, it takes either 1 or -1 . We can see that $C_d(\alpha)$ shows the change of the band Chern number C across the transition point by varying α . For the case of $C_d = 0$, the change of C is zero when varying α , which indicates a topologically trivial phase transition. On the other hand, the case

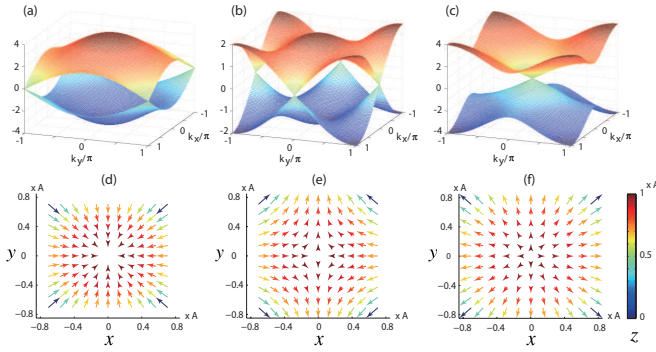


FIG. 5: (Color online) (a)-(c) The energy spectrum of the QWZ model with $\beta = 1$, (a) $\mu = -2$, (b) $\mu = 0$ and (c) $\mu = 2$, respectively. (d)-(f) display the direction of the Hamiltonian \mathbf{h} in the x - y plane, corresponding to the gap closing points in (a)-(c) respectively. In (e) we only display the direction of Hamiltonian around one of gap closing points at $(k_x = \pi, k_y = 0)$ shown in (b), while the other one at $(k_x = 0, k_y = \pi)$ has exactly opposite direction in both the x and y direction.

of $C_d = \pm 1$ corresponds to a topological phase transition from the trivial (topological) phase to topological (trivial) phase. Particularly, when $M = 0$ and $\alpha = 0$ (or π), there are two gap closing points in the Brillouin zone, and the change of C is ± 2 when varying α , which corresponds to the summation of C_d around these two points.

If we choose M as the third parameter besides the momentum \mathbf{k} by keeping α fixed and define $M = M_0 + z$ with $M_0 \mp 3\sqrt{3}\sin\alpha = 0$, the expansion of the Hamiltonian becomes:

$$h(\mathbf{k}) = \mp \sqrt{3}t_1x\sigma_x + t_1y\sigma_y + z\sigma_z, \quad (13)$$

and the Chern number around the gap closing point of \mathbf{K}_+ (\mathbf{K}_-) is always $C_d(M) = -1$ (1), as shown in Fig.4(b). The value of $C_d(M)$ also indicates the change of C when varying M . When $M = 0$ and $\alpha = 0$ and π , the change of C is zero, which also matches the summation of $C_d(M)$.

To visualize the Chern number C_d , we show the direction of $h(\mathbf{k})$ around the gap closing point with different α_0 in Fig.4(c)-(e). One can see that all the arrows point to $z = 0$ in (c), and to the opposite direction in (e), but the z -component of $h(\mathbf{k})$ in (d) is always positive. The value of C_d is associated with the direction of $h(\mathbf{k})$. In Fig.4(c), the direction of $h(\mathbf{k})$ is always toward $x = z = 0$ and away from $y = 0$, which corresponds $C_d = 1$. In Fig.4(e), the direction of $h(\mathbf{k})$ is opposite to the one in Fig.4(c) only in the z direction, corresponding to $C_d = -1$. However, in Fig.4(d), the z -component of $h(\mathbf{k})$ follows the same direction, corresponding to $C_d = 0$.

Our theory can be applied to study other 2D Z-type topological systems with the topological invariant characterized by the Chern number. To give an additional example, we next investigate a lattice model on a square lattice described by the Hamiltonian $H = \mathbf{h} \cdot \boldsymbol{\sigma}$ with $\boldsymbol{\sigma} = (\sigma_x, \sigma_y, \sigma_z)$ the Pauli matrices and $\mathbf{h} = (\sin k_x, \sin k_y, \beta[\mu - \cos k_x - \cos k_y])$, which is known as the Qi-Wu-Zhang (QWZ) model²⁷. Depending on the value of μ , this model has three different topological phases charac-

terised by the band Chern number C . Setting $\beta = 1$, the band Chern number $C = 0$ while $|\mu| > 2$, and $C = -\text{sgn}(\mu)$ when $|\mu| < 2$. There are three phase transition points for this model: $\mu = -2$, $\mu = 0$ and $\mu = 2$. As shown in Fig.5(a)-(c), when $\mu = \pm 2$, there's only one gap closing point ($k_x = k_y = \pi$ for $\mu = -2$ and $k_x = k_y = 0$ for $\mu = 2$) in the Brillouin zone, but when $\mu = 0$, there are two gap closing points ($k_x = \pi, k_y = 0$ and $k_x = 0, k_y = \pi$). By choosing μ as the third parameter beside the momentum, the expansion of the Hamiltonian near the gap closing points results in

$$\begin{aligned} h(\mathbf{k}) &= -x\sigma_x - y\sigma_y + z\sigma_z, \quad \mu = -2; \\ h(\mathbf{k}) &= \pm x\sigma_x \mp y\sigma_y + z\sigma_z, \quad \mu = 0; \\ h(\mathbf{k}) &= x\sigma_x + y\sigma_y + z\sigma_z, \quad \mu = 2. \end{aligned}$$

In Fig.5(d)-(f) we show the direction of \mathbf{h} in the x - y plane, as the z direction of $h(\mathbf{k})$ is always away from $z = 0$. The result shows that $C_d = 1$ for $\mu = \pm 2$, and $C_d = -1$ for both gap closing points when $\mu = 0$, hence the summation of C_d at each phase transition point also corresponds to the change of the band Chern number C .

III. SUMMARY AND OUTLOOK

In summary, we proposed a scheme to study the topological properties of phase transition point for various topological QPTs by introducing a topological invariant defined on a closed curve in the parameter space surrounding the transition point. By studying several typical topological models, we demonstrated that the topological or trivial phase transition can be distinguished by the introduced topological invariant around the transition point, which takes nontrivial quantized numbers for topological QPTs but non-universal numbers or zero number for conventional QPTs. Our theory provides a way to discriminate topological or trivial QPTs by directly studying the properties of the phase transition point.

In order to give a proper definition to the topological invariant of a phase transition point, we have introduced the phase transition driving parameter as an additional dimension parameter besides the momentum space, and thus raise the effective parameter dimension by one. Such an idea seems to share some similarities with the construction in the analysis of topological phases by dimension extension through introducing an additional dynamical parameter²⁸⁻³¹. While the topological invariant is defined in the enlarged $(D + 1)$ -dimensional parameter space for D -dimensional systems in previous works²⁸⁻³¹, in the present work the topological invariant is defined on a close curve of $(D + 1)$ -dimensional space surrounding the phase transition point and thus is effectively defined on a D -dimensional curve. This is the main difference from the previous construction via dimension extension. While our scheme can be applied to Z-type topological systems, it can not be directly generalized to deal with the Z_2 -type systems as the corresponding topological invariant is described by the Z_2 number¹⁷. It would be interesting to study how to characterize the topological phase transition for Z_2 -type systems by analysing the topological property of the phase transition point in the future work.

Acknowledgments

S. C. would like to thank H. M. Weng for helpful discussions. The work is supported by NSFC under Grants No.

11425419, No. 11374354 and No. 11174360.

-
- * Electronic address: schen@aphy.iphy.ac.cn
- ¹ S. Sachdev, *Quantum Phase Transitions*, (Cambridge University Press, Cambridge, England, 1999).
 - ² M. Z. Hasan and C. L. Kane, *Rev. Mod. Phys.* **82**, 3045 (2010).
 - ³ X.-L. Qi and S.-C. Zhang, *Rev. Mod. Phys.* **83**, 1057 (2011).
 - ⁴ G. E. Volovik, *The Universe in a Helium Droplet* (Oxford University Press, Oxford, 2003).
 - ⁵ A. C. M. Carollo and J. K. Pachos, *Phys. Rev. Lett.* **95**, 157203 (2005).
 - ⁶ S. L. Zhu, *Phys. Rev. Lett.* **96**, 077206 (2006); A. Hamma, arXiv:quant-ph/0602091.
 - ⁷ P. Zanardi and N. Paunkovic, *Phys. Rev. E* **74**, 031123 (2006).
 - ⁸ W. L. You, Y. W. Li, and S. J. Gu, *Phys. Rev. E* **76**, 022101 (2007); S. J. Gu, *Int. J. Mod. Phys. B* **24**, 4371 (2010).
 - ⁹ H. Q. Zhou and J. P. Barjaktarevic, *J. Phys. A: Math. Theor.*, **41** 412001(2008).
 - ¹⁰ S. Chen, L. Wang, Y. Hao, and Y. Wang, *Phys. Rev. A* **77**, 032111 (2008); S. Chen, L. Wang, S. J. Gu, and Y. Wang, *Phys. Rev. E* **76**, 061108 (2007).
 - ¹¹ L. Campos Venuti and P. Zanardi, *Phys. Rev. Lett.* **99**, 095701 (2007); P. Zanardi, P. Giorda, and M. Cozzini, *Phys. Rev. Lett.* **99**, 100603 (2007).
 - ¹² Y. Q. Ma, S. Chen, H. Fan, and W. M. Liu, *Phys. Rev. B* **81**, 245129 (2010).
 - ¹³ S. Matsuura and S. Ryu, *Phys. Rev. B* **82**, 245113 (2010).
 - ¹⁴ S.-Q. Shen, *Topological Insulators* (Springer-Verlag, Heidelberg, 2013).
 - ¹⁵ D. J. Thouless, M. Kohmoto, M. P. Nightingale, and M. den Nijs, *Phys. Rev. Lett.* **49**, 405 (1982).
 - ¹⁶ W. P. Su, J. R. Schrieffer and A. J. Heeger, *Phys. Rev. Lett.* **42**, 1698 (1979).
 - ¹⁷ A. Altland and M. Zirnbauer, *Phys. Rev. B* **55**, 1142 (1997); A. P. Schnyder, S. Ryu, A. Furusaki, A. W. W. Ludwig, *Phys. Rev. B* **78**, 195125 (2008); A. Kitaev, *AIP Conf. Proc.* **1134**, 22 (2009).
 - ¹⁸ S. Ryu and Y. Hatsugai, *Phys. Rev. Lett.* **89**, 077002 (2002).
 - ¹⁹ M. Creutz, *Phys. Rev. Lett.* **83**, 2636 (1999).
 - ²⁰ A. Bermudez, D. Patan, L. Amico, and M. A. Martin-Delgado, *Phys. Rev. Lett.* **102**, 135702 (2009); L. H. Li and S. Chen, *EPL*, **109**, 40006 (2015).
 - ²¹ J. Zak, *Phys. Rev. Lett.* **62**, 2747 (1989).
 - ²² D. Xiao, M. C. Chang and Q. Niu, *Rev. Mod. Phys.* **82**, 1959 (2010).
 - ²³ P. Delplace, D. Ullmo, and G. Montambaux, *Phys. Rev. B* **84**, 195452 (2011).
 - ²⁴ T. L. Hughes, E. Prodan, and B. A. Bernevig, *Phys. Rev. B* **83**, 245132 (2011); C.-K. Chiu, H. Yao, and S. Ryu, *Phys. Rev. B* **88**, 075142 (2013).
 - ²⁵ F. D. M. Haldane, *Phys. Rev. Lett.* **61**, 2015 (1988).
 - ²⁶ M. V. Berry, *Proc. R. Soc. London, Ser. A* **392**, 45 (1984).
 - ²⁷ X. L. Qi, Y.-S. Wu, and S.-C. Zhang, *Phys. Rev. B* **74**, 085308 (2006).
 - ²⁸ L.-J. Lang, X. Cai, and S. Chen, *Phys. Rev. Lett.* **108**, 220401 (2012); Y. E. Kraus, Y. Lahini, Z. Ringel, M. Verbin, and O. Zeitlinger, *Phys. Rev. Lett.* **109**, 106402 (2012).
 - ²⁹ Z. H. Xu, L. H. Li, and S. Chen, *Phys. Rev. Lett.* **110**, 215301 (2013); P. Marra, R. Citro, and C. Ortix, *Phys. Rev. B* **91**, 125411 (2015).
 - ³⁰ F. Zhang, C. L. Kane, and E. J. Mele, *Phys. Rev. Lett.* **111**, 056403 (2013).
 - ³¹ E. Prodan, *Phys. Rev. B* **91**, 245104 (2015).